

# Atomic force microscopy for the measurement of flexibility of single softwood pulp fibres

N. Navaranjan · R. J. Blaikie · A. N. Parbhu ·  
J. D. Richardson · A. R. Dickson

Received: 10 March 2008 / Accepted: 4 April 2008 / Published online: 17 April 2008  
© Springer Science+Business Media, LLC 2008

**Abstract** A new method based on the atomic force microscope has been developed to measure the lateral flexibility of single wood pulp fibres. In this method, individual wet pulp fibres from earlywood and latewood of *Pinus radiata* were placed on a newly designed two-point support, and the load and the deflection of fibres were measured under three-point bending test using a modified cantilever probe. The lateral flexibility values of the fibres were then calculated using propped cantilever beam theory. The results obtained indicate that earlywood fibres are substantially more flexible, and have a greater range of flexibility values than latewood fibres.

## Introduction

Atomic force microscope (AFM) has become a very valuable tool in materials science applications. It was originally designed as an imaging tool, but was later modified to be operated in the force mode. Its high sensitivity imaging and force measuring capability has enabled studies of physical–chemical properties of materials at micro- and nanoscale. Remarkably, AFM has been used in measuring the mechanical properties of biomaterials at

even single molecular level. For example, force and compliance measurements on living cells were done at molecular level [1]. Guhados et al. [2] measured the elastic modulus of bacterial cellulose using the force–volume mode, in which the force and deflection of a bacterial fibre that was suspended over a groove were measured at nanoscale and then the elastic modulus was determined using the suspended beam theory of mechanics. Pang and Gray [3] studied the fibrillation effect of pulp fibre surfaces using AFM images. Nilsson et al. [4] used the AFM to measure the conformability (compressibility) of wet pulp fibre surfaces. They placed a wet fibre sample on a flat surface and applied a force using a standard cantilever and probe. The deflection and the force in the transverse direction of the fibre were measured and the conformability was then determined.

Wet fibre lateral flexibility (wet fibre flexibility in pulp and paper literature [5, 6]) or its inverse stiffness is an important fundamental property that contributes to the ability of fibres to deform and entangle during wood pulp processing and papermaking. Fibre flexibility influences flocculation of fibres, drainage and retention characteristics, as well as the structure and properties of paper. Fibres that have high stiffness increase the network strength of low concentration of pulp slurries since they exert greater normal and frictional forces on each other. In order to bond the fibres in a sheet, fibres are brought into contact by flow and capillary forces during sheet drainage and by external pressure during pressing. The more flexible the fibres, the denser and more highly bonded the sheet. Less flexible or stiff fibres are suitable for reinforcing biofibre composites. The flexibility of pulp fibres is also a contributing factor in traditional measurements of pulp freeness and water retention. As this is an important property, measurement of the lateral flexibility of individual fibres has long been of

---

N. Navaranjan (✉) · J. D. Richardson · A. R. Dickson  
Papro, Scion, Private Bag 3020, Rotorua, New Zealand  
e-mail: Namasivayam.Navaranjan@scionresearch.com

R. J. Blaikie  
The MacDiarmid Institute, University of Canterbury,  
Private Bag 4800, Christchurch, New Zealand

A. N. Parbhu  
Industrial Research Limited, Lower Hutt, New Zealand

interest to scientists and engineers [5]. In theory, determining lateral flexibility is not complex, since a single fibre can be considered as either a cantilevered beam or a beam which is subjected to three-point bending. However, measuring the fibre deflection and the load that are required to determine the flexibility is not trivial at microscale, especially when the fibres are wet. Steadman and Young [6] reported a method to determine the fibre flexibility based on producing a very low-density sheet dried over 25  $\mu\text{m}$  diameter parallel stainless steel wires on a glass slide. This method cannot be used effectively for short length fibres or mechanical pulp fibres that do not bond to a glass slide. Furthermore, the span length of the deflected fibre cannot be measured accurately and any minor error can cause significant error in the flexibility calculation as the flexibility is inversely proportional to third order of the span length. Tam Doo and Kerekes [7] published a method where a single fibre was placed across the notched tip of a submerged capillary tube and water was drawn into the tube to deflect the fibre. Kuhn et al. [8] measured the flexibility from the deformation of fibres in a defined hydrodynamic flow field. These two methods have not become popular because setting up a controlled flow field to measure fibre deflections is not an easy and cost-effective task. However these methods could potentially be adapted to provide an online fibre flexibility test device.

The difficulties associated with currently available methods for measuring fibre lateral flexibility led to the development of a new method based on the AFM. In our method, the lateral flexibility of individual fibres of earlywood and latewood radiata pine pulp was measured under a three-point bending test as this is the most convenient method for using the AFM. Nevertheless, using the AFM for this measurement is not straightforward and required a significant amount of development work. Here, we report the procedures developed for obtaining both the force and deflection measurements from the AFM to determine the lateral flexibility under three-point bending. The need to develop a special grooved slide to hold the fibres is discussed along with the need to develop a modified calibrated cantilever to improve the accuracy of the force and deflection measurements.

## Materials and methods

### Fibre preparation

Fibre preparation was done according to the method developed by Kibblewhite et al. [9]. Radial wood strips, 5–7 mm in width and 18–30 mm in depth, were cut from discs of a specific supplied *Pinus radiata* log and the earlywood/latewood boundaries marked with a scalpel prior to

pulping. The strips were secured between perforated stainless steel plates to prevent them from disintegrating during pulping and the clamped strips then placed vertically in a 6 L M/K digester and surrounded by wood chips prior to adding the pulping liquor. They were then kraft pulped using white liquor prepared from reagent grade sodium hydroxide and sodium sulphide with a slow heat up to permit even penetration and diffusion of the liquor into and out of the strips. Pulping conditions were: 20% effective alkali charge (as  $\text{Na}_2\text{O}$ ), 28.1% sulphidity, 8:1 liquor:wood, digester heated to 170 °C over 180 min and then held at 170 °C for 180 min. On completion of the cook, the strips in the screen plates were first rinsed and then soaked overnight in fresh water after which the earlywood/latewood boundary marks were easily distinguishable, allowing relatively easy separation of the earlywood and latewood fibres of each ring with a surgical scalpel. Approximately 300 unbleached, undried and undamaged wet fibres of each pulp type were used for the flexibility measurements.

### Two-point fibre support

A single fibre that is subjected to three-point bend test should be placed on a two-point support. To facilitate this type of support a groove was made by gluing two half-slides on to another glass slide. The typical cross-sectional view of the groove with a fibre is shown in Fig. 1. The width of the groove,  $L$ , was precisely maintained at 0.6 mm while gluing. A wet fibre was placed across the groove. One end of the fibre was fixed using double-sided adhesive tape to prevent any movement during handling and testing.

This setup is similar to a propped cantilever beam which has one end clamped and the other end freely supported. A concentrated load was applied at the centre of the span length of the fibre and the load ( $P$ ) and deflection ( $\delta$ ) were measured using the AFM as explained in the following

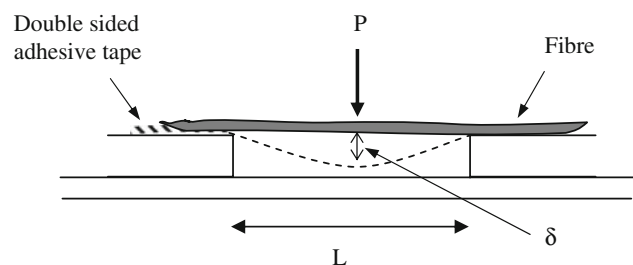


**Fig. 1** Section of the grooved glass slide with double-sided adhesive tape fixing the fibre at one end. The load,  $P$ , applied at the centre of the span length of the fibre deflects the fibre by  $\delta$  across the span length,  $L$

sections. The lateral flexibility,  $F$ , which is the inverse stiffness,  $S$ , is defined as

$$F = 1/S = 1/EI \tag{1}$$

where  $E$  is the modulus of elasticity and  $I$  is the second moment of area. From the beam theory of mechanics [10], the flexibility can be derived under the condition of a statically indeterminate propped cantilever beam for small deflections, and is given by

$$F = \frac{768\delta}{7PL^3} \tag{2}$$

where  $L$  is the span length which is equal to the width of the groove. This equation was used to calculate the flexibility of the fibres.

### AFM instrumentation

The AFM used consists of NanoScope IIIa controller and Dimension 3100 Scanning Probe Microscope System. A cantilever is attached to the Z Piezo of the microscope head which can extend and retract vertically according to the set voltage range. Figure 2 shows a schematic diagram of Z Piezo, cantilever, laser light beam path and position sensitive detector in the Dimension 3100 microscope head.

The Dimension 3100 AFM can be used with either the tapping mode or the contact mode. The first mode is generally used for imaging and the second is used for force measurement. For the flexibility measurement, the grooved glass slide with a wet fibre was placed on the specimen stage of the microscope and secured under vacuum. The fibre on the slide was brought into focus. Under the contact mode, the Z Piezo was then extended to bring the cantilever probe in contact with the fibre by adjusting the Z scan voltage on the AFM. After the probe had contacted the

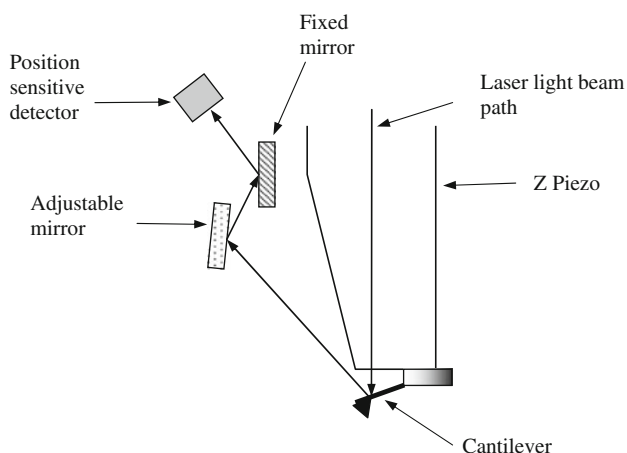


**Fig. 2** Schematic diagram of Z Piezo setup in Dimension 3100 microscope head showing the position of cantilever and path of the laser beam

fibre, further extension of the Z Piezo caused both the fibre and the cantilever to deflect. Figure 3 shows a schematic representation of the fibre and the cantilever deflection.

The fibre deflection,  $\delta$ , was determined from the Z Piezo extension and the cantilever deflection as given by

$$\delta = \Delta z - \Delta c, \quad (\Delta c < \Delta z) \tag{3}$$

where  $\Delta z$  is the distance travelled by Z Piezo and  $\Delta c$  is the deflection of cantilever.

There are different types of cantilevers available with triangle or beam shapes for different applications. The end of a conventional cantilever generally has a sharp conical or pyramid shape probe with the cone angle in the range of 20° and the height of 15–20 μm as shown in Fig. 4a. The conventional probe was found to embed itself in the fibre surface when the force measurement was performed. This embedding adversely affected the flexibility measurement.

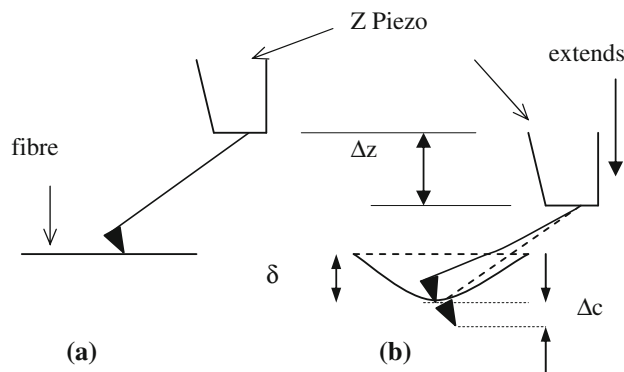
To avoid this problem and have a probe with a well-defined surface area, as shown in Fig. 4b, a glass bead with the diameter of 36.2 μm was attached to a MikroMasch Silicon NSC14 calibrated tipless cantilever with the spring constant of 9.2 N/m and the length of 125 μm. All measurements were performed using this modified probe with the resonant frequency of 160 kHz. In the actual setup, the axis of the fibre was perpendicular to the axis of the cantilever as shown in Fig. 5. This setup also avoided the collision of cantilever against the slide while Z Piezo was extending to deflect the fibre.

The force,  $P$ , applied by the probe was calculated from the cantilever deflection,  $\Delta c$ , and the spring constant,  $k$ , of the cantilever using equation,

$$P = k\Delta c. \tag{4}$$

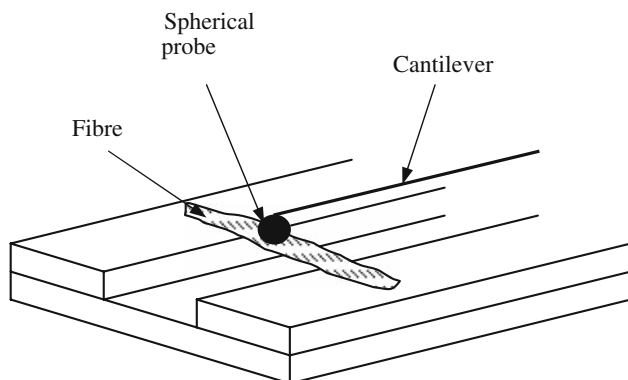
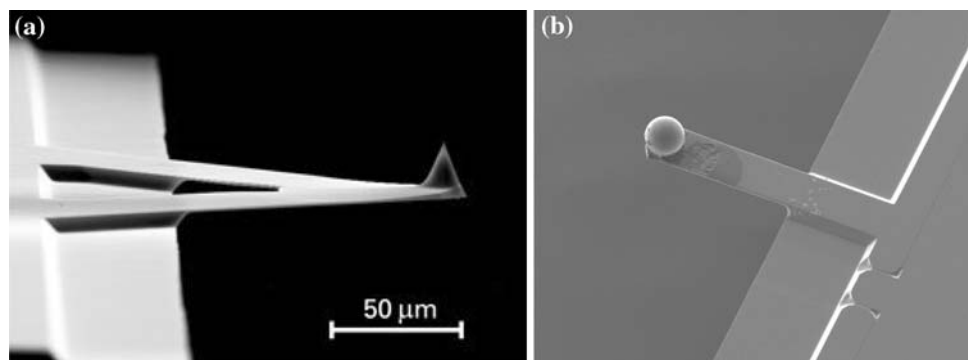
### Typical force curve from the AFM

Figure 6 shows the typical features of an AFM force curve [11]. Figure 7 shows the relative positions of the probe and



**Fig. 3** Schematic diagram of fibre and cantilever (a) before and (b) after deflection. Extension of Z Piezo causes the deflection of both fibre and cantilever

**Fig. 4** (a) Conventional MikroMasch NSC11 triangular cantilever probe and (b) a glass bead probe attached to the calibrated tipless single beam cantilever



**Fig. 5** The axis of a fibre placed on groove is perpendicular to cantilever. Spherical probe prevents embedding into the fibre surface

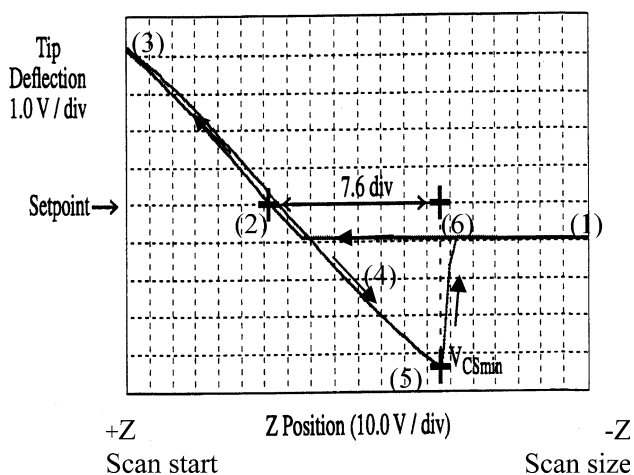


**Fig. 6** Typical force curve from AFM shows the important features [11]

sample for the six points labelled on the curve. The vertical axis of the graph represents the cantilever (tip) deflection voltage while the horizontal axis represents the Z piezo voltage. The Z piezo voltage ranges from +220 V at the extended end to -220 V at the retracted end. The range of the piezo travel is defined by the Z scan start and

Z scan size (see Fig. 6) parameters in the force calibration mode.

The typical force curve represents the deflection signal for one complete extension/retraction cycle of the piezo. From point 1 to 2 there is no change in the deflection signal as the piezo extends, because the probe has not come into contact with the sample. At point 2, the probe contacts the sample and the deflection signal begins to increase. Often, there will be a slight dip in the deflection signal just as the probe reaches the sample surface, because attractive forces between the probe and the sample cause the probe to bend down to the sample surface. Then, the deflection signal continues to increase as the piezo moves the probe down. The deflection signal reaches a maximum at point 3, the maximum piezo extension; then, the piezo starts to retract. The deflection signal decreases as the piezo and the probe retract. At point 4, the cantilever is not deflected, but due to attractive forces between the probe and the sample, the probe sticks to the sample, and the cantilever is pulled down as the piezo continues to retract. Eventually (point 5), the spring force of the bent cantilever overcomes the attractive forces, and the cantilever quickly returns to its non-deflected, non-contact position (point 6).

#### Force curve for a single fibre

The voltage scales of vertical and horizontal axes were converted to the metric length scales and a typical force plot was obtained from the AFM for a single fibre as shown in Fig. 8. The loading (extending) and unloading (retracting) curves are almost coincident and indicate that the fibre responded in an elastic manner. There is no attractive force observed between the probe and the fibre. In cases where the probed position is laterally offset from the midline of the fibre [6], hysteresis in cantilever deflection between the extending and retracting curves was seen and this reading was not considered for flexibility measurement. From the typical force plot, the deflections of the cantilever or tip ( $\Delta c$ ) and the fibre ( $\Delta z$ ) are 103 nm and 3.5  $\mu\text{m}$ , respectively.

**Fig. 7** Piezo travel direction and positions for the typical force curve in Fig. 6 [11]

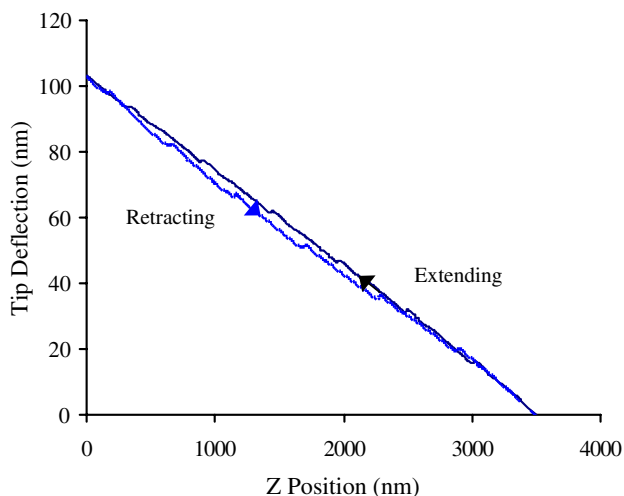
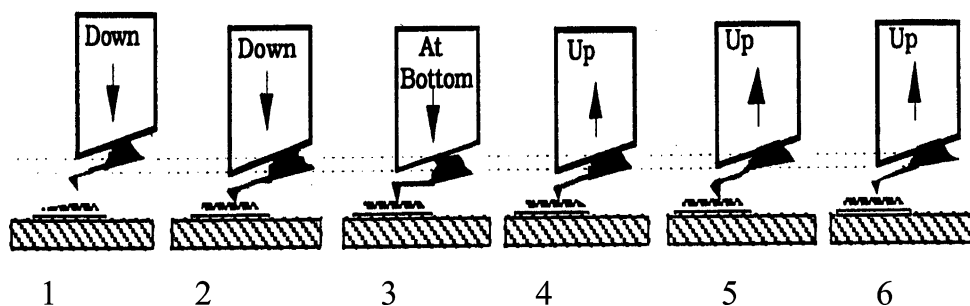


**Fig. 8** Force plot for loading and unloading of a single fibre

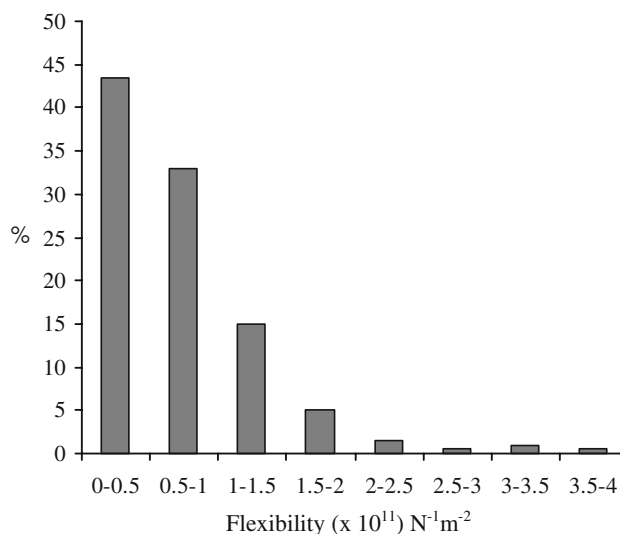


**Fig. 9** Lateral flexibility of latewood fibres: percentage of fibre in a  $0.5 \times 10^{11} \text{ N}^{-1} \text{ m}^{-2}$  flexibility range

**Results**

Cross sections of the fibres that were measured for flexibility were examined using a confocal laser scanning microscope to confirm the fibres were appropriately classified as either type latewood or earlywood. The lateral flexibility data of 200 fibres of each fibre type, latewood and earlywood, are compared in Figs. 9 and 10, respectively.

The average values of the flexibility for latewood and earlywood are  $0.73 \times 10^{11}$  and  $5.49 \times 10^{11} \text{ N}^{-1} \text{ m}^{-2}$ , respectively. The flexibility data of latewood and earlywood have the standard deviation of  $0.59 \times 10^{11}$  and  $3.81 \times 10^{11} \text{ N}^{-1} \text{ m}^{-2}$ , respectively. Flexibility of latewood fibres varies in a narrow range below  $4.0 \times 10^{11} \text{ N}^{-1} \text{ m}^{-2}$  with 44% of fibres having flexibility less than  $0.5 \times 10^{11} \text{ N}^{-1} \text{ m}^{-2}$ . In contrast, flexibility of earlywood fibres varies in a wide range up to  $18.0 \times 10^{11} \text{ N}^{-1} \text{ m}^{-2}$  with 17% of fibres falling in between 2.5 and  $3.0 \times 10^{11} \text{ N}^{-1} \text{ m}^{-2}$  flexibility.

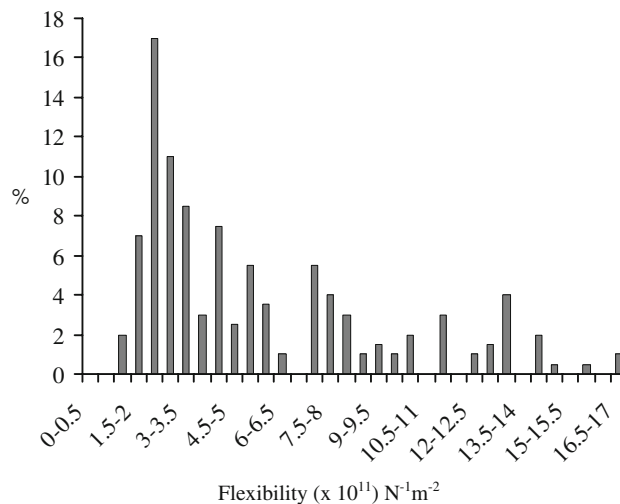


**Fig. 10** Lateral flexibility of earlywood fibres: percentage of fibre in a  $0.5 \times 10^{11} \text{ N}^{-1} \text{ m}^{-2}$  flexibility range

**Discussion**

The lateral resolution of the AFM allows mechanical properties to be determined in samples of nano- and

micrometer size. As reported in [2] elastic modulus of single bacterial cellulose fibres was measured accurately at nanoscale by means of three-point bending test, in which the fibre was clamped at both ends and an AFM cantilever

was used to apply a known force on the fibre. This setup is similar to our method although the wood fibre was clamped at one end and the flexibility was measured at microscale. All flexibility measurements were made with the same calibrated cantilever probe to avoid any errors associated with different probes having different elastic behaviours or there being differences in the shear force effect between the fibre and glass bead. The equation used in this study to calculate the flexibility values is based on the assumption that the fibre was being deformed within its elastic limit under pure bending. Consequently, AFM was only used to induce small deflections (maximum 4  $\mu\text{m}$ ) in the fibre to minimise possible errors in the flexibility numbers. It is possible to use the step-down motor of the AFM to subject the fibre to larger deformations than were examined in this study. However, larger deformations would most likely have exceeded the elastic limit and entered into the viscoelastic region. A small deflection bending test also has the advantage that it minimises the shear force effect between a fibre and the cantilever probe when the force is applied. In principle, the deflection of a fibre is due to tensile, compressive and shear deformations. Waterhouse and Page [12] studied the shear deformation of collapsed and uncollapsed fibres from different test methods and found that there was a considerable shear effect if the test span is short. However, if the test span (0.6 mm) is long like in our method when compared to the width of a fibre (in the order of 50  $\mu\text{m}$ ), the effect of the shear deformation is negligible. Furthermore, the load was applied at the centre of the span length of all the fibres. When the repeatability of loading and unloading was examined, each fibre responded elastically and produced similar force plot. This procedure ensures the consistency of using AFM in this method. The beaded cantilever probe did not appear to embed itself in the fibre surface suggesting that this modification should have further improved the accuracy of lateral flexibility measurements.

Wood fibres have tubular geometry, as like any other soft thin-walled tube subjected to deflection, fibres may kink, buckle or collapse at the loading point. But, in our method, when each fibre was monitored during the test using a video camera that was attached to the AFM, there was no kink or buckling observed in any of those fibres tested. The combination of small deflection of fibre, long test span and distributed load by the spherical probe on the fibre surface would have avoided this problem as well as

the fibre wall damage due to wrinkling effect on the compression side of the fibre. Some earlywood and latewood fibres were placed on a glass slide and load was applied on individual fibres to collapse the fibres in the transverse direction. The force that is required to collapse a fibre was found to be much higher than the force required to deflect the fibre under the three-point bending test. This ensures that the load applied to each fibre would have deflected rather than collapsed the fibre.

All the fibres were kept wet until testing with the AFM had been completed. This ensured that the fibre moisture content was kept above the fibre saturation point. Another advantage of using wet fibre is that the larger cross-sectional dimension (width) of the fibre will tend to lie on the grooved slide due to the higher surface tension force between the fibre and the slide. In future, this procedure could be improved by obtaining a specimen holder for the AFM that enables the fibre to be immersed in water.

The length of the fibres ranges from 1.5 to 4.5 mm. The load was applied at the centre of the span length of all fibres and the span length was constant as the width of the groove is 0.6 mm. This procedure ensures that the uniform tubular length of a fibre with the larger perimeter would have been subjected to the flexibility measurement since Eq. 2 was derived for a uniform statically indeterminate propped cantilever beam. In cases where the probed position is laterally offset from the midline of the fibre or the fibre would have not been perfectly laid on the slide, a hysteresis in cantilever deflection between the extending and retracting curves was seen and this reading was not considered for flexibility measurement.

The earlywood kraft pulp fibres are shown to be more flexible than the latewood kraft pulp fibres. The difference in the range of the flexibility data for the earlywood and the latewood fibre types can be explained based on the collapsibility of the fibres. As the lateral flexibility is inversely related to the product of modulus of elasticity ( $E$ ) and second moment of area ( $I$ ), any decrease in the second moment of area due to fibre collapse will give an increase in flexibility, assuming that the elastic modulus remains unchanged. The second moment of area is dependent on the distribution of the cross-sectional area about the longitudinal axis of the fibre. Figure 11 shows the cross sections of dried latewood fibre and earlywood fibre. Because of the fibre geometry and processing, the earlywood fibre shows the higher degree of collapse. Dried

**Fig. 11** Cross sections of dried (a) latewood kraft pulp fibre and (b) earlywood kraft pulp fibre





fibres generally have slightly different geometries than never-dried fibres. However, these differences are insignificant compared to the differences between earlywood and latewood shown in Fig. 11.

As uncollapsed earlywood fibres have a larger perimeter than latewood fibres, they might be expected to have a similar second moment of area to latewood fibres even though they have thinner fibre walls. However, the larger perimeter and thinner walls of the earlywood fibres also mean that they are more likely to collapse than the smaller perimeter and thicker walled latewood fibres. Fibre collapse generally occurs at a weak point or a defect which is commonly a thinner wall region. Consequently, a wide range of flexibilities is to be expected for the earlywood fibres as those that remain uncollapsed will have a high  $I$  value and low flexibility, whereas those that are collapsed due to the sample preparation processes will have a low  $I$  value and high flexibility. In contrast, the thicker walls of the latewood fibres mean that the sample preparation processes are unlikely to have a major influence on the degree of fibre collapse, and hence, a much smaller range of flexibilities would be expected.

## Conclusions

In summary, the AFM has been shown to be a very useful tool for single fibre lateral flexibility measurements. The results suggested that earlywood fibres were more flexible than latewood kraft fibres. The modified cantilever probe avoided embedding into the fibre surface. The specially designed large span two-point support for three-point bending test minimised the shear deformation in the fibre. The small deflection of fibre during the test minimised the shear force effect between the fibre and the probe. Further

investigation is in progress to develop a relationship among accurately calculated second moment of area, modulus of elasticity and the flexibility, and the results will be reported in the future.

**Acknowledgements** We would like to acknowledge Dr. John Smail of the Department of Mechanical Engineering, University of Canterbury, Christchurch, New Zealand, for his support in preparation of the grooved glass slide. We would also like to thank Dr. Lloyd Donaldson and John Lloyd of Scion, Rotorua, New Zealand, for the SEM micrograph of the beaded cantilever probe and advice with the kraft pulping, respectively.

## References

1. Wojcikiewicz EP, Zhang X, Moy VT (2004) Biological procedures online 6(1). [www.biologicalprocedures.com](http://www.biologicalprocedures.com). Medline. doi: 10.1251/bpo67
2. Guhadós G, Wankei W, Hutter JL (2005) J Am Chem Soc 127:6642. Published online: <http://pubs.acs.org/cgi-bin/abstract.cgi/lang5/2005/21/i14/abs/la0504311.html>
3. Pang L, Gray DG (1998) J Pulp Paper Sci 24(11):369
4. Nilsson B, Wagberg L, Gray D (2001) Conformability of wet pulp fibres at small length scales. 12th Fundamental research symposium, Oxford, September 2001. p 211
5. Lawryshyn YA, Kuhn DCS (1996) J Pulp Paper Sci 22(11):423
6. Steadman RK, Young JH (1972) Paper Technol 10(10):311
7. Tam Doo PA, Kerekes RJ (1982) Pulp Paper Can 83(2):T37
8. Kuhn DCS, Lu X, Olson JA, Robertson AG (1995) J Pulp Paper Sci 21(10):337
9. Kibblewhite RP, Riddell MJC, Sherman LO (2004). Fibre length and wood colour variation in three *radiata* pine discs having varying level of compression wood. Proceeding, 58th Appita Annual Conference, Canberra, Australia
10. Gere JM, Timoshenko SP (1995) Mechanics of materials, 3rd SI edition. Chapman & Hall, NY
11. Instruction Manual (1997) Dimension 3100 scanning probe microscope. Veeco Digital Instruments
12. Waterhouse JF, Page DH (2004) Nord Pulp Paper Res 19(1):89. doi:10.3183/NPPRJ-2004-19-01-p089-092